Viburnum Sargentii Koehne Fruit Extract As Corrosion Inhibitor For Mild Steel In Acidic Solution

Xiumei Wang[*], *Yichong Wang, Qing Wang, Ye Wan, Xiaoqi Huang, Chen Jing*

School of Materials Science and Engineering, Shenyang Jianzhu University, Shenyang, Liaoning, China 110168
[*]E-mail: xmwang@alum.imr.ac.cn

The inhibition effect of Viburnum sargentii Koehne fruit extract (JMG) on mild steel corrosion in 1 M HCl solution was studied by weight loss measurement, electrochemical impedance spectroscopy (EIS) and potentiodynamic polarization curves. The results show that the inhibition effect has a relationship with the dosage of JMG. The inhibition efficiency increases as the concentration of JMG increases and exhibits the opposite trend with an increment in the temperature. The maximum inhibition efficiency reaches 93.8% with the addition of 2.0% JMG at 303 K (weight loss results). JMG inhibits the anodic and cathodic processes simultaneously, and E_{corr} does not change with the increasing concentration, indicating JMG exhibits mixed-type inhibition behavior. The adsorption process of JMG obeys the Langmuir isotherm model, which is an exothermic physisorption accompanied by a decrease in entropy. The activation energy determines the corrosion rate of mild steel in 1 M HCl solution.

1. INTRODUCTION

Mild steel is widely used in various industrial fields due to its low price and physicochemical properties, but it is inevitable that various degrees of corrosion occur in different environments, especially in acidic environments (Oil and gas well acidization, pipeline boiler systems, acid descaling, etc). A simple and economical corrosion inhibitor technology has become the most important method to protect mild steel against corrosion. Among different types of corrosion inhibitors, organic inhibitors that have S, P, O, N and multiple bonds in their structures exert good corrosion inhibition effects [1-18]. However, a large number of organic inhibitors are toxic and cause harm to environment and human beings. Therefore, some toxic and harmful inhibitors are prohibited from use. In view of

protecting environment, the development of efficient corrosion inhibitors that are nonpoisonous and environment friendly is a potential and ideal research area.

In recent years, there have been some reports on natural product extracts as mild steel inhibitors [19-27]. Plant extracts are considered as a wide source of naturally synthesized chemical compounds. Usually, a natural product extract contains several ingredients, and it is difficult to determine the specific component that has corrosion resistance properties. The excellent inhibition effect is ascribed to the synergism of a variety of components [28]. Viburnum Sargentii Koehne is widely cultivated in many countries including China, Canada, and America. It is mainly used for landscaping and has an oval, red, juicy fruit with thin skin. Viburnum Sargentii Koehne fruit contains flavonoids, linoleic acid, kaempferol and other compounds containing heteroatoms, which are consistent with the structural characteristics of corrosion inhibitor. The extract of Viburnum Sargentii Koehne fruit as corrosion inhibitor has not been reported and has numerous advantages such as abundant material sources, low cost, friendly to environment and simple extract procedures.

In this paper, the inhibition effect of Viburnum Sargentii Koehne fruit extract (JMG) was investigated as a novel, nontoxic, environment friendly corrosion inhibitor for mild steel in 1.0 M HCl solution by weight loss measurements, electrochemical impedance spectroscopy (EIS) and potentiodynamic polarization, and the results and inhibition mechanism are analyzed and discussed.

2. EXPERIMENTAL

2.1 Materials

The composition (mass%) of mild steel strips used in this investigation is as follows: 0.12 C, 0.061 Si, 0.52 Mn, 0.005 P and the remainder Fe. Samples with the size 10 mm × 10 mm × 3 mm were applied for weight loss experiments. For electrochemical measurements, the working electrode was a cube with a side length of 1 cm and the other parts were covered with epoxy resin with a 1 cm^2 surface area exposed to corrosive solution. The 1.0 M HCl solution was made by adding distilled water to analytical reagent-grade 37% HCl. The volume of the corrosive solution was 200 mL.

2.2 Extraction of JMG

Viburnum sargentii Koehne fruits were collected in winter in Shenyang, China. The fruits were juiced by a squeezer for 10 minutes at room temperature without addition of water, chemicals or other reagents. Then, the juice was obtained by filtering and removing solid residue. The juice (JMG) is employed as corrosion inhibitor for mild steel directly, and the concentration of JMG is expressed as a percentage (0.08%, 0.20%, 0.40%, 0.80%, and 2.0%). The whole extraction procedure is very simple, nontoxic and economical compared to other extractprocedures since many extraction procedures require the use of some organic and inorganic chemicals, heat and reflux [29-35].

2.3 Weight loss measurements

Weight loss measurements were performed in 300 mL capacity flasks with 200 mL of the corrosive solutions. Before measurements, the samples were abraded by 100-800 grit emery paper to obtain a bright mirror surface, rinsed and cleaned with distilled water, greased with ethanol, dried and stored in a vacuum desiccator. The samples were immersed and suspended in the corrosive media with the help of rod and hook for 5 h at 303 K-333 K in a thermostatic water bath. After immersion, the corroded mild steel samples were rinsed with distilled water, and the corroded product was wiped off with alcohol-soaked cotton and dried. The specimens were accurately weighed ($\pm$ 0.1 mg) by an analytical balance before and after immersion. The corrosion rate (V), inhibition efficiency ($IE\%$) and coverage (θ) were calculated by formulas (1), (2), and (3), respectively:

$$V = \frac{W - W_0}{s \times t} \qquad (1)$$

where V is the corrosion rate, mg cm^{-2} h^{-1}; W_0 and W are the weight loss values of the mild steel coupon before and after immersion, respectively, in mg; s is the corrosion area of mild steel samples in cm^2 and t is the corrosion time in h.

$$IE\% = \frac{V_0 - V_{inh}}{V_0} \times 100\% \qquad (2)$$

$$\theta = \frac{V_0 - V_{inh}}{V_0} \qquad (3)$$

where V_0 and V_{inh} are the corrosion rates of mild steel in the 1.0 M HCl solution without and with the addition of different concentrations of JMG, respectively.

2.4 Electrochemical measurements

Electrochemical studies were performed on a Parstat 2273 electrochemical workstation at 303 K in a conventional three-electrode cell; a Pt sheet of 1 cm×1 cm and a saturated calomel electrode (SCE) were employed as the auxiliary and reference electrodes, respectively. The exposed surface area of the working electrode was 1 cm^2 (except for the working surface, the other parts were encapsulated in epoxy resin). The reference electrode was connected to a Luggin capillary. All the potentials reported are with reference to SCE. The working electrode surface was polished to 800# with a variety of emery papers, cleaned with distilled water, scrubbed with alcohol-soaked cotton, dried and kept in a vacuum desiccator. Before the experiments, the working electrode was soaked in the corrosive media for nearly 0.5 h until the open-circuit potential (OCP) was constant.

The potentiodynamic polarization curves were carried out in the range from -150 mV to + 200 mV (vs. OCP) at a scanning rate of 0.5 mV s^{-1}. Electrochemical impedance spectroscopy (EIS) was performed by applying a sinusoidal voltage with 10 mV amplitude at the OCP of the working electrode across the frequency range 100 kHz-10 mHz. In each run, a fresh working electrode was employed. Three to five runs were conducted for each test to acquire reliable and reproducible results.

The experimental data analysis was performed using Cview and Zview.

3. RESULTS AND DISCUSSION

3.1 Weight loss measurements

Fig. 1 shows the change in the corrosion inhibition efficiency (*IE%*) for mild steel as a function of the JMG concentration at 303 K, 313 K, 323 K and 333 K.
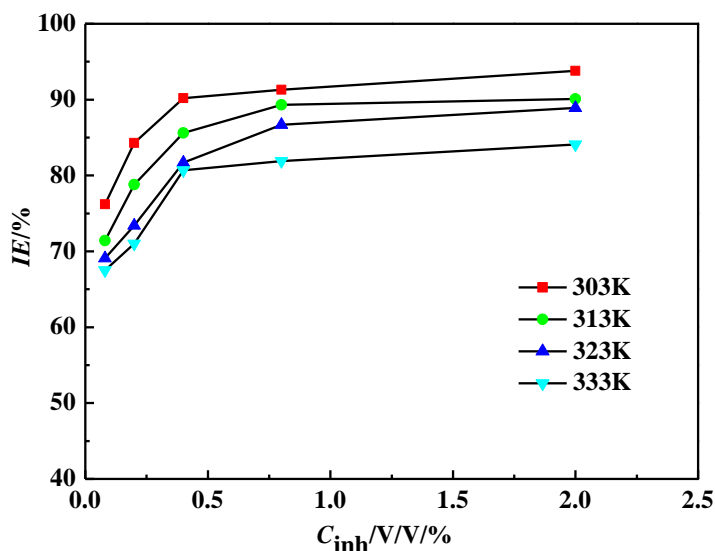
Figure 1. Relationship between corrosion inhibition efficiency (*IE%*) and JMG concentration at different temperatures (303-333 K) in 1M HCl solution.

The obtained results (Fig. 1) suggest that within the studied concentration range, the corrosion inhibition efficiency is proportional to JMG concentration and inversely proportional to the temperature. The inhibition efficiency increased with enhanced JMG concentration. This fact can be explained by more adsorption of JMG organic components on the mild steel surface, which increases the mild steel surface coverage and suppresses the corrosion rate [36].

Once the concentration is higher than 0.4%, the inhibition efficiency of JMG shows a little change, which represents almost saturation of JMG adsorption on the mild steel surface. With the addition of the same JMG concentration, the *IE%* decreases with the increasing temperature, which is the result of an increase in JMG desorped from the metal surface. The maximum value, 93.8%, of *IE%* is obtained with 2% JMG at 303 K.

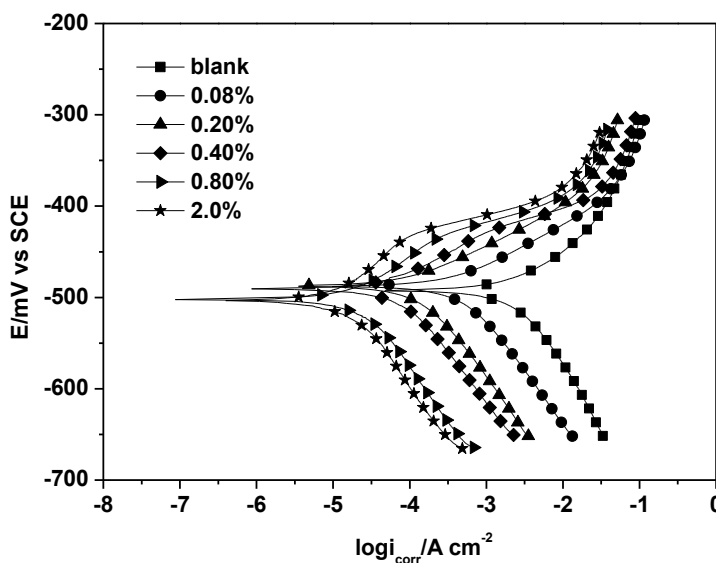### 3.2 Potentiodynamic polarization curves

Fig. 2 shows the anodic and cathodic potentiodynamic polarization curves of a mild steel electrode in blank 1 M HCl solution with various concentrations of JMG at 303 K. Fig. 2 shows that both the cathodic and anodic curves shifts to lower current densities with the addition of JMG compared to that recorded in blank solution, and the anodic and cathodic current densities show further decrease as JMG concentration is increased, indicating JMG inhibits both anodic and cathodic

corrosion processes of mild steel simultaneously [37]. Since the JMG extract with complex composition contains a variety of organic components with polar functional groups, different components may interact by mutual repulsion or attraction and be adsorbed on the anodic and cathodic sites of the mild steel surface to retard the anodic and cathodic corrosion processes [28].

The electrochemical parameters obtained by extrapolation of the Tafel curve, i.e., the corrosion potential (E_{corr}), corrosion current density (i_{corr}), anodic (β_a) and cathodic (β_c) Tafel slope, are shown in Table 1. The corrosion inhibition efficiency (*IE%*) of JMG is also listed in the Table 1 calculated by the following formula (4) [39].

$$IE_{(i)}\% = \frac{i_{corr}^0 - i_{corr}^{inh}}{i_{corr}^0} \qquad (4)$$

where i^o_{corr} and i^{inh}_{corr} are the corrosion current densities of mild steel electrodes in uninhibited and inhibited solutions, respectively.

Figure 2. Potentiodynamic polarization curves of a mild steel electrode in 1 M HCl solution without and with various concentration of JMG at 303 K.

Table 1. Extrapolation results of potentiodynamic polarization curves and calculated *IE%*.

C_{inh} /V/V/%	E_{corr} /mV *vs* SCE	i_{corr} /μA cm^{-2}	β_a /mV dec^{-1}	β_c /mV dec^{-1}	*IE* /%
blank	491	1460	93	108	-
0.08	481	539	97	112	63.1
0.20	479	352	90	103	75.9
0.40	472	136	95	107	90.7
0.80	498	102	102	106	93.0
2.0	502	67	98	115	95.4

Table 1 shows the corrosion inhibition efficiency increases and the corrosion current density decreases with the increment of JMG concentration. The best inhibition occurred at a JMG concentration of 2.0%, and the maximum inhibition efficiency reached 95.4%. The results of the inhibition efficiencies obtained by polarization technique are in agreement with those calculated from weight loss data. The slight differences are due to method error. The E_{corr} values did not obviously change with and without different concentrations of JMG. The maximum shift in the E_{corr} value was 30 mV, which confirmed that JMG acts as a mixed-type inhibitor [40]. The JMG adsorption on mild steel surface is geometric coverage effect, and the coverage degree is equal to the corrosion inhibition efficiency [41]. Table 2 also reveals JMG has a little influence on the anodic (β_a) and cathodic (β_c) Tafel slopes, indicating that JMG may not change the mechanisms of the cathodic reaction and anodic dissolution [42]. The inhibition mechanism of JMG is that JMG adsorbs on the mild steel surface due to a synergistic effect of multiple components to form a compact film, which prevents the corrosive solution to reach mild surface; thus, the corrosion current density is decreased significantly and corrosion inhibition is enhanced.

3.3 EIS Results

Fig. 4 shows the Nyquist plots of mild steel electrodes in 1 M HCl solutions in the absence and presence of different concentrations of JMG at 303 K. As seen, the impedance response of mild steel in 1 M HCl significantly changed after the addition of JMG. The Nyquist plots of mild steel electrodes in 1 M HCl medium with addition of JMG have similar shapes to that in blank solution, but the size increases as the JMG concentration is increased. This indicates that the impedance of mild steel increases with the increase in JMG concentration, and correspondingly, the inhibition efficiency is enhanced. The Nyquist plots show a depressed capacitive loop, which might be due to inhomogeneities on the electrode surface, the time constant of charge transfer and double layer capacitance [43]. This suggests that the corrosion reaction of mild steel electrode is controlled by the charge transfer process and does not change with the addition of JMG. The capacitance loop is related to the charge transfer process of mild steel corrosion and double layer behavior [44]. Meanwhile, the size of capacitive loops in Fig. 3 increase with the addition of JMG. This result indicates that the inhibition efficiency (*IE*) is proportional to the concentration of JMG. The EIS results are consistent with weight loss results.

An equivalent circuit displayed in Fig. 3 was used to fit the Nyquist plots [45]. In general, a Randles circuit is selected to analyze interactions at the interface of a metal/solution. The circuit is composed of solution resistance (R_s), charge transfer resistance (R_{ct}) and double layer capacitance (C_{dl}). The imperfect capacitive loops result from frequency dispersion, which can be attributed to the nonhomogeneity of mild steel electrode surface. Therefore, constant phase angle component (*CPE*) is introduced to displace the double layer capacitance, C_{dl}, to describe the real capacitive behavior. The value of *CPE* consists of the double layer capacitance, C_{dl}, and a diffusion coefficient, *n*.

The fitting results and corrosion inhibition efficiency (*IE*%) calculated according to the charge transfer resistance are all listed in Table 2.

$$IE_{(R)}\% = \frac{R_{ct}^{inh} - R_{ct}^{o}}{R_{ct}^{inh}} \times 100\% \tag{5}$$

where R_{ct}^{o} and R_{ct}^{inh} are the charge transfer resistances of mild steel electrode in 1 M HCl solutions in the absence and presence of different concentrations of JMG at 303 K, respectively.
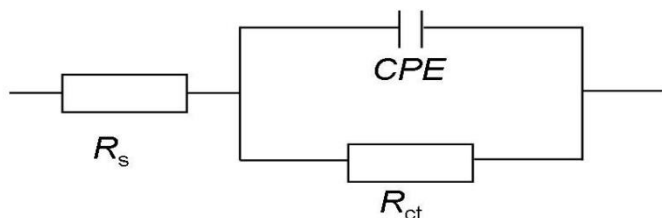

Figure 3. Equivalent circuit used to model the experimental results.

Table 2. Electrochemical parameters obtained by EIS.

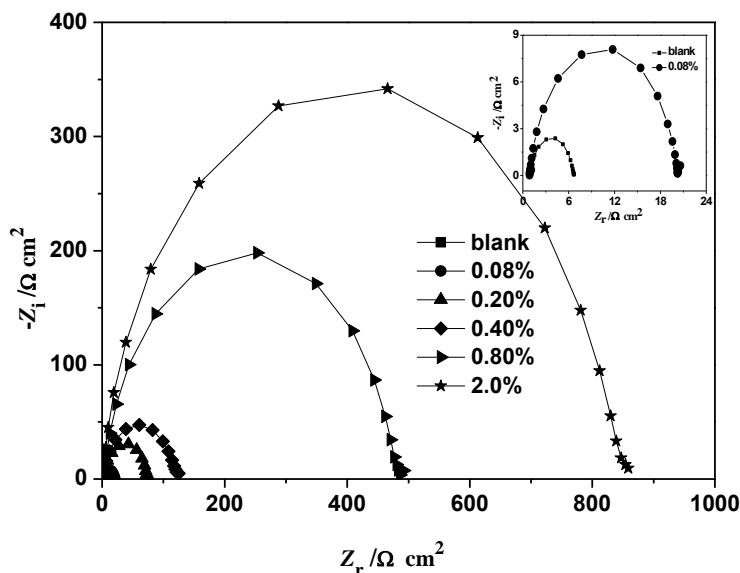| C_{inh} /V/V/%	R_s /Ω cm^2	CPE /C_{dl}/μF cm^{-2}(n)		R_{ct} /Ω cm^2	IE /%
blank	1.2	962	(0.90)	5	-
0.08	1.1	373	(0.87)	18	72.2
0.20	2.8	189	(0.89)	71	93.0
0.40	1.4	126	(0.92)	118	95.8
0.80	2.3	89	(0.88)	484	99.0
2.0	2.6	68	(0.91)	845	99.4

Figure 4. Nyquist plots of mild steel in 1 M HCl solution without and with different concentrations of JMG at 303 K.

Table 2 shows that the R_{ct} values were enhanced and the C_{dl} values were reduced in the presence of JMG, which may be due to the adsorption of JMG onto the metal/solution interface to displace H_2O molecules. This adsorption enables a JMG protective film to form on the mild steel surface, preventing the corrosion reaction [46-47]. Additionally, the decreased C_{dl} value can be ascribed to the decrease in the dielectric constant and increase in the thickness of the electrical double layer [48]. The displacement ratio increases as the JMG concentration increases, and the inhibition efficiency is enhanced as a result. The maximum calculated value of the inhibition efficiency is 99.4%. The high inhibition efficiency also clarifies that JMG can form a compact adsorption layer and cover the metal surface [49]

3.4 Adsorption isotherm and thermodynamic parameters
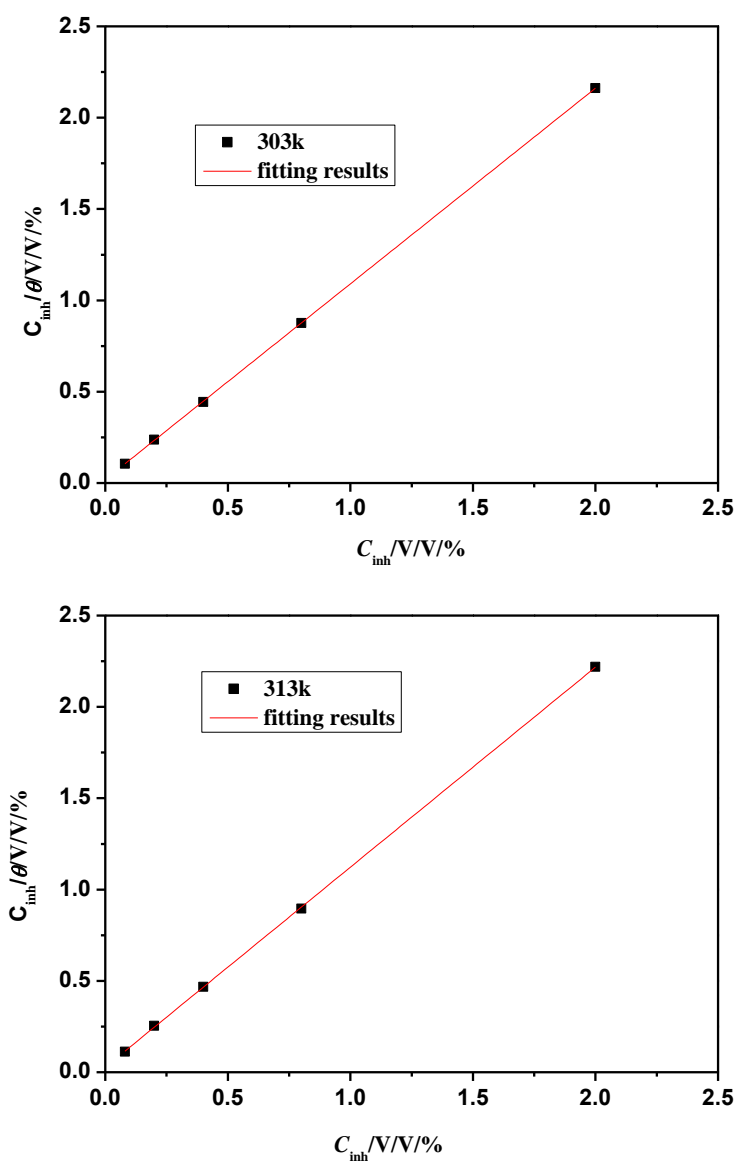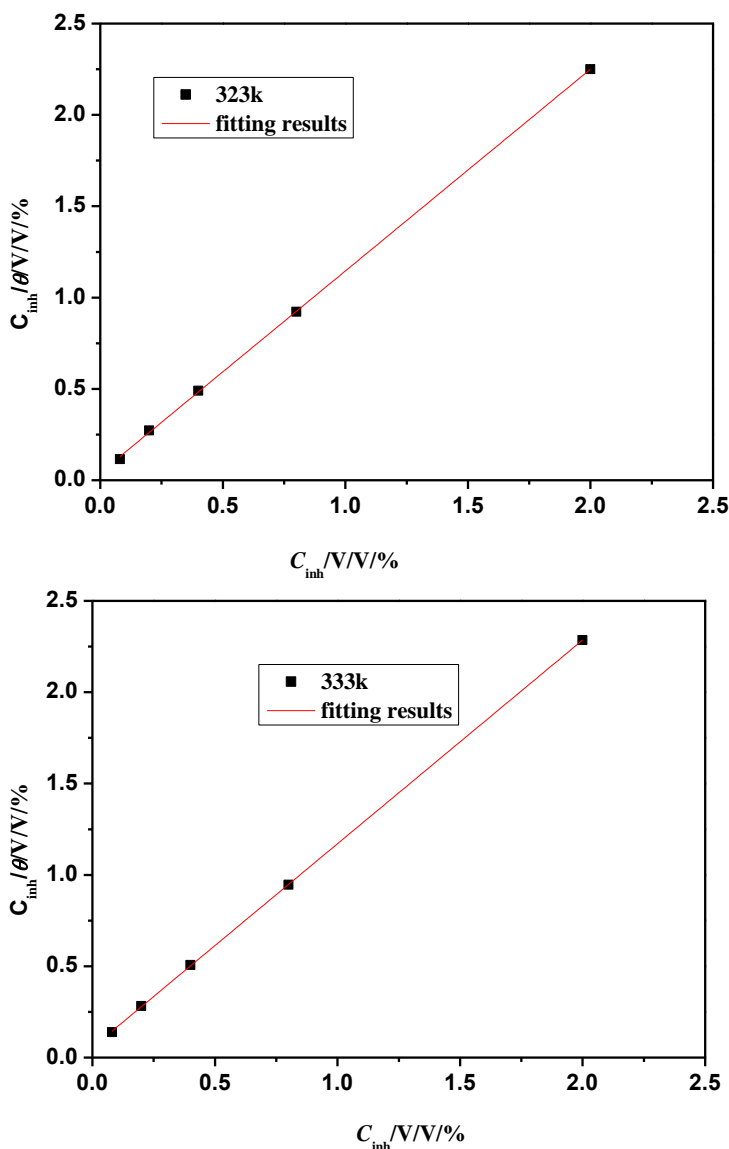
Figure 5. Langmuir adsorption isotherm and fitting results at different temperatures (303-333K).

Supposing that the adsorption mechanism of JMG is described by Langmuir adsorption model, then, the coverage of JMG on mild steel surface should be equal to the corrosion inhibition efficiency since JMG is a mixed-type inhibitor (based on the weight loss results). The coverage was fitted by Langmuir adsorption isotherm. The results indicate that Langmuir isotherm is a good fit for the experimental results. The Langmuir isotherm is shown in formula (6).

$$\frac{C_{inh}}{\theta} = C_{inh} + \frac{1}{K_{ads}} \qquad\qquad (6)$$

where C_{inh} represents that concentration of JMG (V/V%), θ represents the surface coverage, and K_{ads} represents the adsorption equilibrium constant.

Fig. 5 shows the plots of C_{inh}/θ versus C_{inh} for JMG at 303 K, 313 K, 323 K, and 333 K. The plots are linear with slopes close to 1 (1.07 at 303 K, 1.09 at 323 K, 1.10 at 323 K, and 1.12 at 303 K)

and high regression coefficients (>0.999), suggesting JMG adsorption on mild steel surface conforms to Langmuir adsorption isotherm. The slopes slightly deviated from the theoretical value of 1, which may be due to the interactions of adsorbed species on the mild steel surface. Since JMG contains some organic compounds with polar atoms, various components adsorbed on the active sites of the mild steel surface may interact with each other through mutual attractive or repulsive forces [50-51].

The intercepts for the plots of C_{inh}/θ versus C_{inh} were used to calculate the adsorption equilibrium constants, and the adsorption equilibrium constant is related to the Gibbs free energy as described in formula (7):

$$K_{ads} = \frac{1}{C_{solvent}} \exp(\frac{-\Delta G_{ads}^{o}}{RT})$$

(7)

where R is the molar gas constant, J mol^{-1}·K^{-1}; T is the absolute temperature, K; K_{ads} is the adsorption equilibrium constant; ΔG^{o}_{ads} is the Gibbs free energy, kJ mol^{-1}; and $C_{solvent}$ is the concentration of water in solution. The unit of $C_{solvent}$ is determined by the unit of K_{ads}. As seen in Table 3, K_{ads} does not have units, and consequently, $C_{solvent}$ is 1.0.
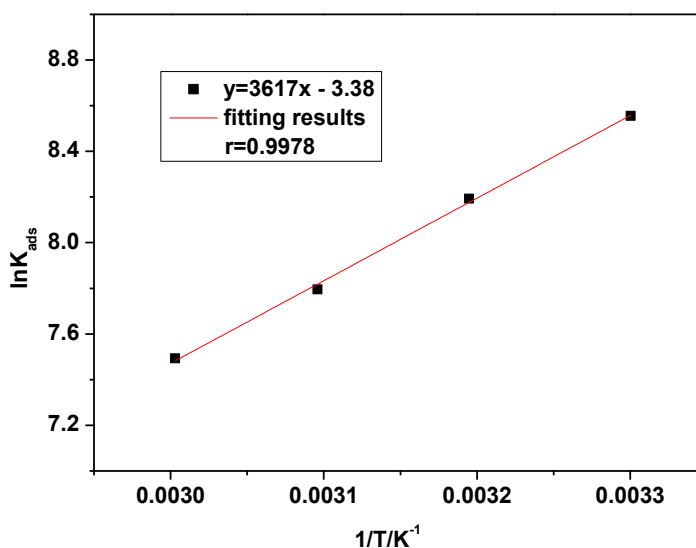
Figure 6. Straight line of ln K_{ads} versus $1/T$ and fitting results.

A negative value of ΔG^{o}_{ads} indicates a spontaneous inhibitor adsorption process and guarantees the stability of the adsorption film on metal surface. The stability of the adsorption film decreased with the increase in temperature gradually [52]. Generally, negative values of ΔG^{o}_{ads} around 20 kJ mol^{-1} or lower, are considered as physical adsorption, and those that are close to 40 kJ mol^{-1} or higher involve chemisorption [53-54]. Accordingly, the values of ΔG^{o}_{ads} calculated for JMG at different temperature are 21.6 kJ mol^{-1} at 303 K, 21.3 kJ mol^{-1} at 313 K, 20.9 kJ mol^{-1} at 323 K, and 20.7 kJ mol^{-1} at 333 K. The ΔG^{o}_{ads} values decrease with the increment of temperature. These results indicate that JMG adsorption mechanism on a mild steel surface may be attributed to spontaneous physisorption.

The thermodynamic parameter the standard adsorption enthalpy, ΔH_{ads}^{o}, can be obtained using the Van't Hoff equation:

.

$$\ln K_{ads} = \frac{-\Delta H_{ads}^{\,o}}{RT} + B \qquad\qquad (8)$$

where R is the gas constant, 8.314 J K^{-1} mol^{-1}; T is the absolute temperature, K; K_{ads} is the adsorption equilibrium constant; and B is the integration constant. In Fig. 6, $\ln K_{ads}$ versus $1/T$ exhibits a straight line with a good linear relationship (r=0.9978). The slope ($\Delta H_{ads}^{\,o}/R$) can be used to calculate $\Delta H_{ads}^{\,o}$, and the value of $\Delta H_{ads}^{\,o}$ is shown in Table 3.

Table 3. Thermodynamic parameters obtained.

T /K	K_{ads}	r	slope	ΔG°_{ads} /kJ mol^{-1}	ΔH°_{ads} /kJ mol^{-1}	ΔS°_{ads} /J mol^{-1} K^{-1}
303	5192	0.99998	1.07	-21.6		-28.1
313	3614	0.99994	1.09	-21.3	-30.1	-28.1
323	2429	0.99984	1.10	-20.9		-28.5
333	1795	0.99997	1.12	-20.7		-28.2

The standard adsorption entropy, ΔS^{o}_{ads}, is calculated using ΔH^{o}_{ads} and ΔG^{o}_{ads} in the following formula (9) and is given in Table 3.

$$\Delta G_{ads}^{\,o} = \Delta H_{ads}^{\,o} - T \times \Delta S_{ads}^{\,o} \qquad\qquad (9)$$

The negative value of $\Delta H_{ads}^{\,o}$ represents an exothermic adsorption process. That means the corrosion inhibition efficiency decreases as the temperature increases. This phenomenon can be explained that the increase in temperature results in an increase in the desorption of JMG from mild steel surface.

In this case, all ΔS^{o}_{ads} values are negative and show little change at the selected temperatures. This suggests the adsorption process is a process accompanied by a decrease in entropy. The negative value of $\Delta H_{ads}^{\,o}$ suggests that JMG adsorption on the mild steel surface is an exothermic process, which is due to physisorption. This is a good explanation that *IE* % decreases with the increase in the temperature in our work.
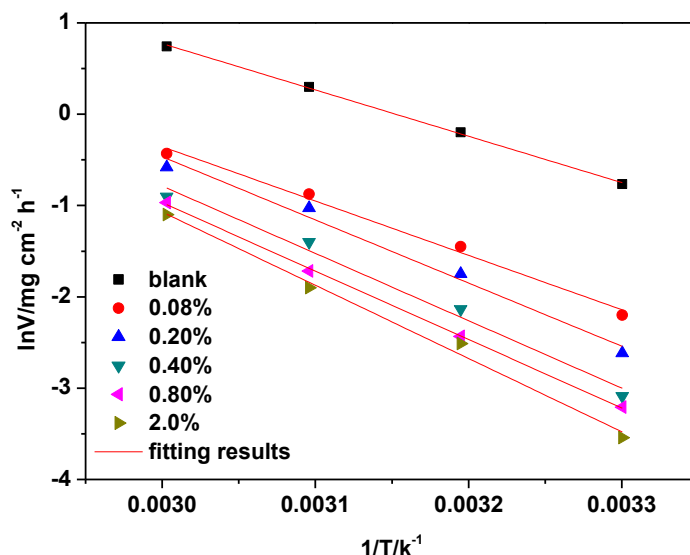
3.5 Kinetic parameters

The Arrhenius equation is

$$\ln V = \frac{-E_a}{RT} + \ln A \qquad (10)$$

where E_a is the apparent activation energy, A is a pre-exponential factor, and V is the corrosion rate.

The Arrhenius equation shows that at a certain temperature, the corrosion rate of metal is determined by the pre-exponential factor, A, and the activation energy, E_a. In general, the influence of the change in E_a on the corrosion rate is greater than that of A. However, A is the decisive factor that affects mild steel corrosion if the change in the A value is far greater than the change in the E_a value.

Fig. 7 shows the Arrhenius plots of ln$V$ versus 1/T of mild steel in the blank 1.0 M HCl and containing various concentrations of JMG. Fig. 7 clearly shows that the corrosion process of mild steel in HCl solution in the absence and presence of JMG follows the Arrhenius equation. The E_a values calculated from the slopes and the A values obtained from intercepts are summarized in Table 4. A decrease in corrosion inhibition efficiency with the increase in the temperature is consistent with a little lower activation energy in blank solution than that in the solution with JMG and may be due to physisorption between the mild surface and JMG [55-56].

Figure 7. Plots of ln$V$ and 1/T for mild steel in 1 M HCl solution in the absence and presence of different concentrations of JMG and the fitting results.

Table 4. Kinetic parameters of mild steel in 1 M HCl solution in the absence and presence of different concentrations of JMG.

C_{inh} /V/V/%	E_a /kJ mol^{-1}	A mg cm^{-2} h^{-1}
blank	42.2	8.7×10^6
0.08	49.5	4.0×10^7
0.20	57.5	6.4×10^8
0.40	61.3	1.8×10^9
0.80	62.3	2.2×10^9
2.0	66.7	9.7×10^9

In Table 4, it is noted E_a values for the mild steel corrosion process in the presence of different concentrations of JMG are higher than that in 1.0 M HCl without JMG. Hence, the corrosion rates decreased. Such high activation energy indicates that JMG is adsorbed on the mild steel surface by weak physisorption. Meanwhile, the E_a value increases with the increasing JMG addition. The increase in E_a might be attributed to JMG adsorption on the mild steel surface to decrease the active sites of the mild steel and slow down the dissolution rate of mild steel. It can be observed in Table 4, the A

value also increased with the increasing JMG concentration (high E_a and low A values result in low corrosion rates according to formula (10)). As seen in Fig. 7, the corrosion rate of mild steel decreases with the increase in JMG concentration gradually; therefore, E_a is the determining factor that influences the corrosion rate of mild steel in a 1 M HCl solution.

4. CONCLUSIONS

(1) Viburnum sargentii Koehne fruit extract (JMG) has good inhibition behavior on mild steel in 1 M HCl solution. The corrosion inhibition efficiency is directly proportional to the concentration of JMG and inversely proportional to the temperature. When the concentration is 2%, the inhibition efficiency is as high as 93.8%.

(2) JMG suppresses both the anodic dissolution of mild steel and the cathodic hydrogen evolution reaction simultaneously, and JMG is a mixed-type inhibitor for mild steel.

(3) In the experimental temperature range, the adsorption of JMG on mild steel follows the Langmiur adsorption isotherm, which is a spontaneous, exothermic, physical adsorption process accompanied by the decrease in entropy.

(4) The activation energy and pre-exponential factor increase with the increase in the JMG concentration, and the activation energy is the determining factor for the corrosion rate of mild steel in 1 M HCl solution.

References

1. A.K. Satapathy, G. Gunasekaran, S.C. Sahoo, K. Amit, P.V. Rodrigues, *Corros. Sci.,* 51 (2009) 2848.
2. C. Kustu, C.K. Emregul, O. Atakol, *Corros. Sci.,* 49 (2007) 2800.
3. D.M. Ortega-Toledo, J.G. Gonzalez-Rodriguez, M. Casales, L. Martinez, A. Martinez-Villafañe, *Corros. Sci.,* 53 (2011) 3780.
4. X.H. Li, S.D. Deng, H. Fu, *Mater.Chem. Phys.,* 129 (2011) 696.
5. S. Ghareba, S. Omanovic, *Electrochim. Acta,* 56 (2011) 3890.
6. M.P. Desimone, G. Grundmeier, G. Gordillo, S.N. Simison, *Electrochim. Acta*, 56 (2011) 2990.
7. X.H. Li, S.D. Deng, H. Fu, *Corros. Sci.,* 53 (2011) 664.
8. El-Sayed M. Sherif, *Mater. Chem.Phys.,*129 (2011) 961.
9. N. Yilmaz, A. Fitoz, C. Emregül., *Corros. Sci.,* 11 (2016) 110.
10. K.G. Zhang, B. Xu, W.Z. Yang, X.S. Yin, Y.Z. Chen, *Corros. Sci.,* 90 (2015) 284.
11. A. Popova, M. Christov, A. Vasilev, *Corros. Sci.*, 94 (2015) 70.
12. G.L. F. Mendonça, S.N. Costa, V.N. Freire, P.N.S. Casciano, P. LimaNeto, *Corros. Sci.,* 115 (2017)41.
13. N. Kıcır, G. Tansuğ, M. Erbil, T. Tüken, *Corros. Sci.,* 105 (2016) 88.

14. Z.Y. Hu, Y.B. Meng, X.M. Ma, H.L. Zhu, D.L. Cao, *Corros. Sci.,* 112 (2016) 563.
15. M. Farsak, H. Keleş, M. Keleş, *Corros. Sci.,* 98 (2015) 223.
16. R. Yıldız, *Corros. Sci.,* 90 (2015) 544.
17. Q. Ma, S.J. Qi, X.H. He, Y.M. Tang, G. Lu, *Corros. Sci.,* 129 (2017) 91.
18. H. Heydari, M. Talebian, Z. Salarvand, K. Raeissi, M.A. Golozar, *J. Mol. Liq.,* 254 (2018) 177.
19. M. Lebrini, F. Robert, H. Vezin, C. Roos, *Corros. Sci.,* 52 (2010) 3367.
20. A.Y. Musa, A.A.H. Kadhum, A.B. Mohamad, M.S. Takriff, *Corros. Sci.,* 52 (2010) 526.
21. M. Elachouri, M.S. Hajii, S. Kertit, E.M. Essasi, *Corros. Sci.,* 37 (1995) 381.
22. M.A. Quraishi, H.K. Sharma, *J. Appl. Electrochem.,* 35 (2005) 33.
23. M. Bouklah, A. Ouassini, B. Hammouti, E. Idrissi, *Appl. Surf. Sci.,* 252 (2006) 2178.
24. E.E. Oguzie, *Corros. Sci.*, 49(2007) 1527.
25. M. Behpoura, S.M. Ghoreishia, M. Khayatkashania, N. Soltani, *Mater. Chem. Phys.,* 131 (2012) 621.
26. A.Y. El-Etre, *Appl. Surf. Sci.,* 252 (2006) 8521.
27. M. Chevalier, F. Robert, N. Amusant, M. Traisnel, M. Lebrini, *Electrochim. Acta,* 131 (2014) 96.
28. K.K. Anupama, K. Ramya, K.M. Shainy, A. Joseph, *Mater. Chem. Phys.,* 167 (2015) 28.
29. P. Parthipan, J. Narenkumar, P. Elumalai, P.S. Preethi, A. Rajasekar, *J.Mol. Liq.,* 240 (2017) 121.
30. A. Saxena, D. Prasad, R. Haldhar, G. Singh, A. Kumar, *J. Environ. Chem. Eng.,* 6 (2018) 694.
31. H. Hassannejad, A. Nouri, *J. Mol. Liq.,* 254 (2018) 377.
32. K. Azzaoui, E. Mejdoubi, S. Jodeh, A. Lamhamdi, H. Lgaz, *Corros. Sci.,* 129 (2017) 70.
33. K.P.V. Kumar, M.S.N. Pillai, G.R. Thusnavis, J. Mater. Sci. Technol., **27** (2011) 1143.
34. H. Gerengi, H.I. Sahin, *J. Ind. Eng. Chem.,* 51 (2012) 780.
35. S. Garai, S. Garai, P. Jaisankar, J.K. Singh, A. Elango, Corros. Sci., 60 (2012) 193.
36. G. Ji , S. Anjum, S. Sundaram, R. Prakash, *Corros. Sci.*, 90 (2015) 107.
37. M. Chevalier, F. Robert, N. Amusant, M. Traisnel, C. Roos, M. Lebrini, *Desalination*, 278 (2011) 337.
38. K.F. Khaled, N. Hackerman, *Electrochim. Acta,* 48 (2003) 2715.
39. A. Zarrouk, B. Hammouti, T. Lakhlifi, M. Traisnel, H. Vezin, F. Bentiss, *Corros. Sci.,* 90 (2015) 572.
40. A.Y. El-Etre, *Mater. Chem. Phys.,* 108 (2008) 278.
41. X.H. Li, S.D. Deng, H. Fu, *Corros. Sci.*, 51 (2009) 1344.
42. P. Kalaiselvi, S. Chellammal, S. Palanichamy, G. Subramanian, *Mater. Chem. Phys.,* 120 (2010) 643.
43. T. Szauer, A. Brandt, *Electrochim. Acta,* 26 (1981) 1253.
44. M. Lebrini, M. Traisnel, L. Gengembre, G. Fontaine, O. Lerasle, N. Genet, *Appl. Surf. Sci.,* 257 (2011) 3383.
45. M.N. El-Haddad, *Int. J. Biol. Macromol.,* 55 (2013) 142.
46. T. Ibrahim, H. Alayan, Y. Al Mowaqet, *Prog. Org. Coat.,* 75 (2012) 456.
47. D.S. Chauhan, K.R. Ansari, A.A. Sorour, M.A. Quraishi, R. Salghi, *Int. J. Biol. Macromol.* 107 (2018) 1747.
48. M.A. Bedair, M.M.B. El-Sabbah, A.S. Fouda, H.M. Elaryian, *Corros. Sci.,* 128 (2017) 54.
49. S. Banerjee, V. Srivastava, M.M. Singh, *Corros. Sci.,* 59 (2012) 35.
50. O. Kaczerewska, R. Leiva-Garcia, R. Akid, B. Brycki, *J. Mol. Liq.,* 247 (2017) 6.
51. F. Bentiss, C. Jama, B. Mernari, H.E. Attari, L.E. Kadi, M. Lebrini, M. Traisnel, M. Lagreneé, *Corros. Sci.,* 51 (2009) 1628.
52. M.A. Amin, M.M. Ibrahim, *Corros. Sci.,* 53 (2011) 873.
53. M. Prabakaran, S.H. Kim, N. Mugila, V. Hemapriya, I.M. Chung, *J. Ind. Eng. Chem. ,* 52 (2017) 235.
54. M. Lebrini, M. Lagrenee, H. Vezin, M. Traisnel, F. Bentiss, *Corros. Sci.,* 49 (2007) 2254.

55. P.E. Alvarez, M.V. Fiori-Bimbi, A. Neske, S.A. Brandán, C.A. Gervasi, *J. Ind. Eng. Chem.,* 58 (2018) 92.
56. A. Popova, E. Sokolova, S. Raicheva, M. Christov, *Corros. Sci.,* 45 (2003) 33.